A multiscale model based on intragranular microstructure - Prediction of dislocation patterns at the microscopic scale

Gérald Franz, Farid Abed-Meraim, Tarak Ben Zineb, Xavier Lemoine, Marcel Berveiller

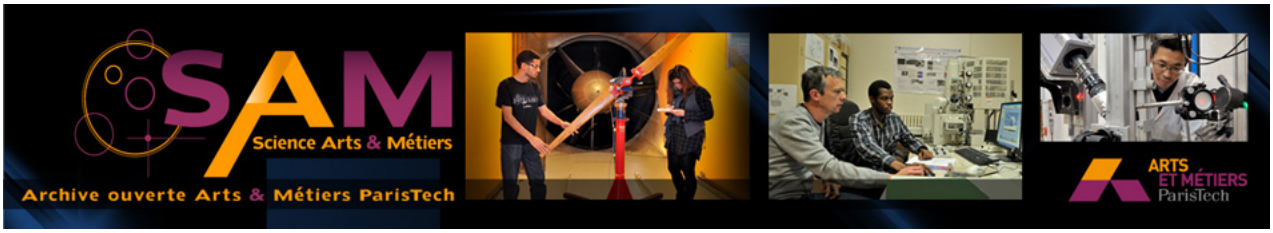

A Multiscale Model Based On Intragranular Microstructure – Prediction Of Dislocation Patterns At The Microscopic Scale

Gérald Franz [1], Farid Abed-Meraim [1], Tarak Ben Zineb [2], Xavier Lemoine [3], Marcel Berveiller [1]

1 LPMM, UMR CNRS 7554, ENSAM 4 rue Augustin Fresnel, 57078 Metz Cedex 3, France
2 LEMTA, UMR CNRS 7563, Nancy Universités 2 rue Jean Lamour, 54519 Vandœuvre-lès-Nancy, France
3 Centre Automobile Produit, Arcelor Research S.A., voie Romaine B.P. 30320, 57283 Maizières-lès-Metz, France

Abstract. A large strain elastic-plastic single crystal constitutive law, based on dislocation annihilation and storage, is implemented in a new self-consistent scheme, leading to a multiscale model which achieves, for each grain, the calculation of plastic slip activity, with help of regularized formulation drawn from visco-plasticity, and dislocation microstructure evolution. This paper focuses on the relationship between the deformation history of a BCC grain and induced microstructure during monotonic and two-stage strain paths.

Keywords: Crystal plasticity, Microstructure, Dislocations, Complex strain paths.

INTRODUCTION

The evolution of the plastic anisotropy of polycrystals during plastic flow can be attributed to several sources taking place at different scales. These include at the mesoscopic scale the slip processes and consequently, the texture and internal stresses development, and at the microscopic scale the development of intragranular dislocations patterns. During sheet metal forming processes, strain-path changes often occur in the material and consequently, some macroscopic effects appear due to the induced plastic anisotropy during the previous deformation. These softening/hardening effects must be correctly predicted because they can significantly influence the strain distribution and may lead to flow localization, shear bands and even material failure. The physical cause of these effects can be associated to the intragranular microstructural evolution. This implies that an accurate description of the dislocations patterning during monotonic or complex strain-paths is needed to lead to a relevant constitutive model. In this paper, a crystal plasticity model coupled with a description of the microstructural evolution at the grain scale is presented. Then the capability of the model to predict at a microscopic scale the evolution of dislocation sheets during changing strain paths will be shown on a simple shear loading and on a reverse test.

SINGLE CRYSTAL MODEL

The elastic-plastic single crystal constitutive law written within the large strain framework presented here can be found in several works [1-3]. The single crystal behaviour is assumed to be elastic-plastic and the plastic deformation is only due to crystallographic slip. The other plastic deformation modes as twinning or phase transformation are not considered. In BCC metals, 24 independent slip systems are potentially active, i.e. the slip planes {110} and {112} and the slip directions <111>.

The velocity gradient, written below g, consists of a symmetric part d corresponding with strain rate of crystalline lattice, and a skew symmetric part w representing the rotation rate:

$$g_{ij} = d_{ij} + w_{ij} \tag{1}$$

Plastic strain and rotation rates can be expressed by introducing the slip rate $\dot{\gamma}$:

$$d_{ij}^{p} = d_{ij} - d_{ij}^{e} = R_{ij}^{g}\dot{\gamma}^{g},\ w_{ij}^{p} = w_{ij} - w_{ij}^{e} = S_{ij}^{g}\dot{\gamma}^{g} \tag{2}$$

where R and S are the symmetric and skew symmetric parts of Schmid tensor.

A slip system is active if its resolved shear stress τ^{g} achieves a critical value τ_{c}^{g} and if its rate $\dot{\tau}^{g}$ reaches the critical shear stress rate value $\dot{\tau}_{c}^{g}$. Consequently, the considered slip rate is different of zero. That can be written as:

$$\begin{aligned} &\tau^{g} < \tau_{c}^{g} \Rightarrow \dot{\gamma}^{g} = 0 \\ &\tau^{g} = \tau_{c}^{g},\ \dot{\tau}^{g} < \dot{\tau}_{c}^{g} \Rightarrow \dot{\gamma}^{g} = 0 \\ &\tau^{g} = \tau_{c}^{g},\ \dot{\tau}^{g} = \dot{\tau}_{c}^{g} \Rightarrow \dot{\gamma}^{g} \neq 0 \end{aligned} \tag{3}$$

To avoid combination analysis and save computing time, the relationship (3) can be expressed by a visco-plastic type regularization, without introducing time dependency. The new formulation is written for a single system g:

$$\dot{\gamma}^{g} = k^{g}\dot{\tau}^{g},\quad k^{g} = \frac{1}{H^{gg}}\left\{\frac{1}{2}\left(1+\tanh\left(k_{1}\left(\frac{\left|\tau^{g}\right|}{\tau_{c}^{g}}-1\right)\right)\right)\right\}\left\{\frac{1}{2}\left(1+\tanh\left(k_{2}\dot{\tau}^{g}\tau^{g}\right)\right)\right\} \tag{4}$$

where H^{gg} is the self-hardening term.

In large strain framework, the elastic law is written as:

$$\hat{\sigma}_{ij} = C_{ijkl}\left(d_{kl} - d_{kl}^{p}\right) - \sigma_{ij}d_{kk} \tag{5}$$

where C is the elasticity tensor and $\hat{\sigma}$ is the Cauchy stress co-rotational derivative. After some mathematical developments, the slip rate expression becomes:

$$\dot{\gamma}^{g} = \left(\delta_{hg} + k^{h}R_{ij}^{h}C_{ijkl}R_{kl}^{g}\right)^{-1}k^{h}R_{ij}^{h}\left(C_{ijkl} - \sigma_{ij}\delta_{kl}\right)d_{kl} \tag{6}$$

where δ is the Kronecker symbol.

The behaviour law is described using a tangent operator linking the nominal stress rate $\dot{n}$ with the velocity gradient g. The single crystal incremental constitutive law is obtained by:

$$\begin{aligned} &\dot{n}_{ij} = l_{ijkl}g_{kl},\ l_{ijkl} = \left[C_{ijkl} - \frac{1}{2}\left(\delta_{ik}\sigma_{lj} + \delta_{il}\sigma_{kj}\right) - \frac{1}{2}\left(\sigma_{ik}\delta_{lj} - \sigma_{il}\delta_{jk}\right)\right] - \\ &\left[C_{ijpq}R_{pq}^{g} + S_{ip}^{g}\sigma_{pj} - \sigma_{ip}S_{pj}^{g}\right]\left[\delta_{hg} + k^{h}R_{mn}^{h}C_{mnpq}R_{pq}^{g}\right]^{-1}k^{h}R_{mn}^{h}\left[C_{mnkl} - \sigma_{mn}\delta_{kl}\right] \end{aligned} \tag{7}$$

MODELING OF INTRAGRANULAR MECHANISMS

This microscopic model, based on experimental observations on BCC grains, is inspired by the works of Peeters [4]. The hardening is described through several families of dislocation densities and their evolution.

During plastic deformation, an intragranular microstructure develops, consisting of straight planar dislocations walls and of statistically stored dislocations in the cells. This microstructure is characterized by three dislocation densities (Figure 1.). The dislocation cells are represented by a single dislocation density for the whole slip systems. Two different dislocation densities are associated with six dislocations walls families: the density of immobile dislocations ρ^{wd} stored in walls, and the polarity dislocation density ρ^{wp}, that is assumed to have a sign.

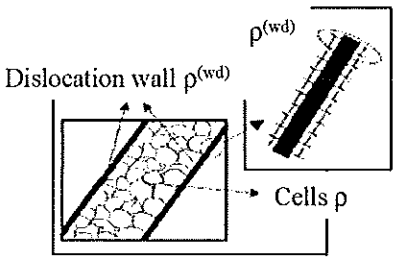

FIGURE 1. Schematic representation of the intragranular microstructure: dislocation sheets parallel to {110} planes of the most active slip systems, cells with a more random character [4].

The model constructs at most two families of walls, in agreement with the experimental observations ; the primary family is generated parallel to the {110}-plane of the most active slip system, the second one is constructed in the same way, parallel to the {110}-plane of the second active slip system. The model distinguishes the evolution of walls created by the current slip processes from the evolution of walls formed by the prior slip activity.

The immobile dislocation density of each current wall i can be calculated by:

$$\dot{\rho}_i^{wd} = \frac{1}{b}\left(I^{wd}\sqrt{\rho_i^{wd}} - R^{wd}\rho_i^{wd}\right)\dot{\Gamma}_i \tag{8}$$

with b the magnitude of the Burgers vector, $\dot{\Gamma}_i$ the total slip rate on the plane of the ith most active slip system and I^{wd} and R^{wd} the immobilization and the recovery coefficients. The last one scales with the annihilation length y_c.

The storage and recovery of polarity dislocations for each current wall i, can be described by:

$$\dot{\rho}_i^{wp} = \left(sign\left(\Phi_i^{wp}\right)I^{wp}\sqrt{\rho_i^{wd} + \left|\rho_i^{wp}\right|} - R^{wp}\rho_i^{wp}\right)\left|\Phi_i^{wp}\right| \tag{9}$$

where $\Phi_i^{wp} = \sum_{s=1}^{n}\frac{\dot{\gamma}^s}{b}m^s n_i^w$ is the net flux of dislocations from slip systems non-coplanar of each current wall i, the scalar product of the unit slip direction vector m^s

of the system s with the normal unit vector n_i^w of the wall i being equal to zero for slip activity coplanar with this wall. I^{wp} and R^{wp} are respectively the immobilization and the recovery coefficients of the polarity dislocations.

When a flux Φ_i^{wp}, associated with a family i of current walls, is reversed (for example during reverse tests), the polarity dislocations stuck at the border of theses walls are annihilated:

$$\dot{\rho}_i^{wp} = -R_{rev}\rho_i^{wp}\left|\Phi_i^{wp}\right| \tag{10}$$

where R_{rev} is the recovery coefficient of the polarity dislocations.

A change in deformation path or a rotation of a crystal can lead to the activation of new slip systems. The mobile dislocations form new walls corresponding to the current deformation mode, but also disintegrate the old walls formed by prior slip activity, according to:

$$\dot{\rho}_i^{wd} = -\frac{R_{ncg}}{b}\rho_i^{wd}\dot{\Gamma}_{new},\ \dot{\rho}_i^{wp} = -\frac{R_{ncg}}{b}\rho_i^{wp}\dot{\Gamma}_{new} \tag{11}$$

where $\dot{\Gamma}_{new}$ denotes the total slip rate on the two crystallographic planes containing the highest slip activity and R_{ncg} the annihilation coefficient of the latent walls.

During reverse tests, a change in deformation path leads to the activation of the same slip systems but in the opposite sense. The polarity dislocations stuck at the border of the walls can move easily away and are annihilated by dislocations of opposite sign in cells. There is an increase of the annihilation rate for the randomly distributed cells:

$$\dot{\rho} = \frac{1}{b}\left\langle\left(I\sqrt{\rho} - R\rho\right)\sum_{s=1}^{n}\left|\dot{\gamma}_s\right| - \Psi R_2\rho\frac{\rho_{bausch}}{2\rho_{sat}^{wp}}\sum_{s=1}^{n}\left|\dot{\gamma}_s\right|\right\rangle \tag{12}$$

with I and R the immobilization and the recovery coefficients of the cells. If no fluxes are reversed $\Psi = 0$, otherwise $\Psi = 1$ with $\rho_{bausch} = \left|\rho_i^{wp}\right|$ if only one flux, corresponding to the family i of wall, is reversed, and $\rho_{bausch} = \sum_{i=1}^{2}\left|\rho_i^{wp}\right|$ if two fluxes are reversed.

The critical shear stress on slip system g includes several contributions: τ_0 represents all aspects of the microstructure that are not included in the internal variables (e.g. initial grain size), τ^{cells} depicts isotropic hardening due to the cells, τ^w introduces the latent hardening of the walls, and takes the contribution of polarity associated to the walls into account. The resultant critical shear stress is given by:

$$\tau_c^g = \tau_0 + (1-f)\tau^{cells} + f\sum_{i=1}^{6}\tau_{ig}^w \tag{13}$$

with

$$\tau^{cells} = \alpha Gb\sqrt{\rho},\ \tau_{ig}^w = \alpha Gb\left(\left\langle m_s.n_i^w sign\left(\rho_i^{wp}\right)\sqrt{\left|\rho_i^{wp}\right|}\right\rangle + \left|m_s.n_i^w\right|\sqrt{\rho_i^{wd}}\right) \tag{14}$$

where α represents the dislocation interaction parameter, G the shear modulus and f the volume fraction of walls.

RESULTS ON A SINGLE CRYSTAL

The parameters given in the Table 1. were used here. These parameters are obtained by fitting the simulated results with five different experimental tests (two reverse tests and two cross tests with different predeformation and a monotonic shear). The values of the material constants used in the model are shown in Table 2. The initial values of the dislocations densities equal 1.10^9 m^{-2}.

TABLE 1. Material parameters [4].

I	R [m]	I^{wd}	R^{wd} [m]	R_{neg} [m]	I^{wp}	R^{wp} [m]	R_{rev} [m]	R_2 [m]
$2,2.10^{-2}$	$8,5.10^{-10}$	$9,4.10^{-1}$	$2,6.10^{-8}$	$2,3.10^{-9}$	$5,0.10^{-2}$	$3,8.10^{-9}$	$1,0.10^{-8}$	$1,0.10^{-8}$

TABLE 2. Material constants [4].

b [m]	G [MPa]	α	f	τ_0 [MPa]
$2,48.10^{-10}$	$8,16.10^4$	0,2	0,2	42,0

In Figure 2 (left) a TEM micrograph in a grain of a specimen after a 15% shear test with shear direction (SD) parallel to rolling direction (RD) is depicted. The traces of only one pronounced family of dislocation wall can be observed, parallel to the (101) slip plane. Figure 2 (right) shows a TEM micrograph in a grain of a specimen after a reverse test with SD parallel to RD. The traces of two pronounced families of dislocation walls can be observed, ones are parallel to the (011) slip plane and the others are parallel to the (10-1) slip plane.

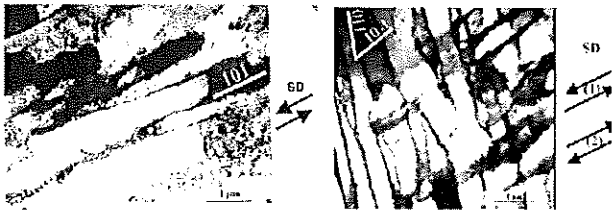

FIGURE 2. TEM micrographs in a grain with initial orientation: (-27.2°, 133.4°, 53°) after a shear test of 15% (left); (43.3°, 127.2°, -43.2°) after a reverse test of -30%/30% (right) [4].

In Figure 3 and Figure 4, the dislocation density ρ^{wd} stored in the walls (left) and the polarity dislocation density ρ^{wp} associated with the walls (right), are depicted as a function of the shear strain γ.

For the simple shear mode, there is only one pronounced family of walls, parallel to (101)-plane, predicted by the model, as it is shown on Figure 3 (left). This result is in agreement with the TEM observation. The polarity dislocation density is low (Figure 3 (right)) because there is only one pronounced activated slip system and the wall is generated parallel to the plane of this system.

For the reverse test, the model predicts the traces of both families of walls (Figure 4 (left)). The decrease of the dislocation density ρ^{wd} at the beginning of the second load, not present in the Peeters simulation results [4], is due to the progressive activation of the slip systems. During the prestrain, the polarity along the walls is

generated, due to the accumulation of dislocations of opposite sign at either side of the walls. During the reversal of the load, the polarity dislocations are mobilized again and are annihilated with dislocations of opposite sign, leading to a depolarization of the walls. After this transition zone, the walls are polarized again, the polarity dislocations are accumulated at the borders of the current walls. These different steps are depicted on Figure 4 (right).

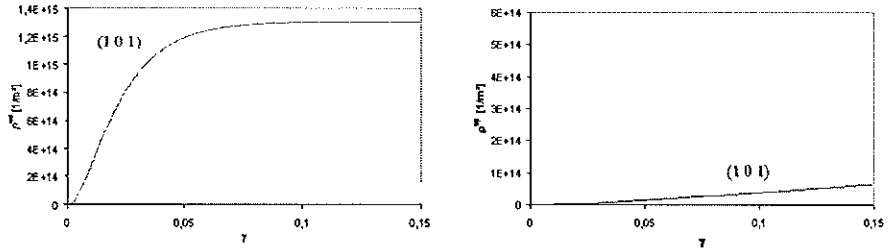

FIGURE 3. Evolution of the intensity and polarity of the dislocation walls in a crystal with initial orientation (-27.2°, 133.4°, 53°) during a shear test.

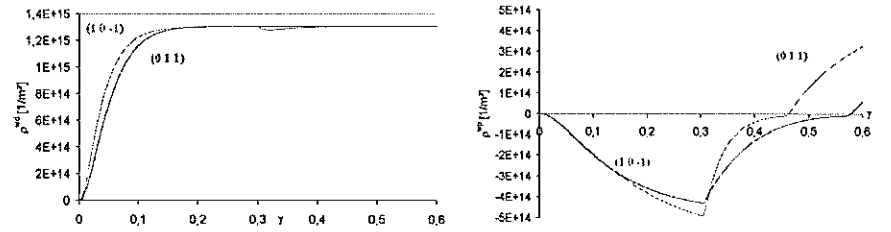

FIGURE 4. Evolution of the intensity and polarity of the dislocation walls in a crystal with initial orientation (43.3°, 127.2°, -43.2°) during a reverse test.

CONCLUSIONS

The present paper shows two examples of intragranular microstructure prediction with the model for a monotonic deformation and two-stage strain paths. Our results are similar to the results obtained by Peeters [4].

The model is validated at the microscopic scale because it is able to reproduce the dislocation microstructure observed in TEM after monotonic deformation, reverse test and cross test (not shown here) for crystal with different initial orientations.

REFERENCES

1. R. J. Asaro, *Journal Of Applied Mechanics* **50**, pp. 921-934 (1983).
2. D. Pierce, R. J. Asaro and A. Needleman, *Acta Metallurgica* **31-12**, pp. 1951-1976 (1983)
3. T. Iwakuma and S. Nemat-Nasser, "Finite Elastic-Plastic Deformation Of Polycrystalline Metals And Composites", Technical rapport 83-3-51.
4. B. Peeters, "Multiscale Modelling Of The Induced Plastic Anisotropy In IF Steel During Sheet Forming", Ph.D. Thesis, Katholieke Universiteit Leuven, 2002